sophisticated theories which account for aerodynamic interaction. However, for configurations with lighter and thinner fuselages, it is believed that the aerodynamic interaction will prove to be more important, and such configurations will require early analysis with an accurate interaction aerodynamic theory.

4) For the successful prediction of the airframe critical flutter mode, the dynamic idealization must realistically include the elastic characteristics of all interactive components.

5) Complete aircraft flutter analyses using component aerodynamics without interaction (i.e., wing and tail aerodynamics separately) should be avoided because such analyses may obscure the potentially critical wing-tail mechanism.

6) A potential wing-tail interaction instability can be prevented by geometric rearrangement, or by considerable structural stiffening, and quite possibly by "active control" with the stabilator control system.

References

[1] Topp, L. J., Rowe, W. S., and Shattuck, A. W., "Aeroelastic Considerations in the Design of Variable Sweep Airplanes," ICAS Paper 66-12, 5th International Council of the Aeronautical Sciences Congress, London, 1966.

[2] Shelton, J. D., Tucker, P. B., and Davis, J. C., "Wing-Tail Interaction Flutter of Moderately Spaced Tandem Airfoils," AIAA Paper 69-57, New York, 1969.

[3] Sensburg, O. and Laschka, B., "Flutter Induced by Aerodynamic Interference Between Wing and Tail," *Journal of Aircraft*, Vol. 7, No. 4, July-Aug. 1970, pp. 319–324.

[4] Mykytow, W. J. et al., "Subsonic Flutter Characteristics of a Variable Sweep Wing and Horizontal Tail Combination," AFFDL-TR-69-59, 1969, Wright-Patterson Air Force Base, Ohio.

[5] Yates, E. C., Jr., "Modified Strip Analysis Method for Predicting Wing Flutter at Subsonic to Hypersonic Speeds," *Journal of Aircraft*, Vol. 3, No. 1, Jan.-Feb. 1966, pp. 25–29.

[6] Falkner, V. M., "The Calculation of Aerodynamic Loading on Surfaces of Any Shape," British RM 1910, 1943, National Physics Laboratory.

[7] "The Development of Subsonic Unsteady Aerodynamics for Wing-Tail Interference," Rept. G246, Vol. 3, May 1968, McDonnell Aircraft Co., St. Louis, Mo..

[8] Rowe, W., "Collocation Method for Calculating the Aerodynamic Pressure Distribution on a Lifting Surface Oscillating in Subsonic Compressible Flow," *AIAA Symposium on Structural Dynamics and Aeroelasticity*, Boston, 1965.

[9] Hsu, P., "Flutter of Low Aspect-Ratio Wings, Part I Calculation of Pressure Distributions for Oscillating Wings of Arbitrary Planform in Subsonic Flow by the Kernel Function Method," ASRL 64-1, 1957, M.I.T., Cambridge, Mass.

[10] Watkins, C. E., Woolston, D. S., and Cunningham, H. J., "A Systematic Kernel Function Procedure for Determining Aerodynamic Forces on Oscillating or Steady Finite Wings at Subsonic Speeds," TR R-48, 1959, NASA.

[11] Ashley, H., Widnall, S., and Landahl, M., "New Directions in Lifting Surface Theory," *AIAA Journal*, Vol. 3, No. 1, Jan. 1965, pp. 3–16.

MAY 1971 J. AIRCRAFT VOL. 8, NO. 5

Advanced Design Concepts for Buckling-Critical Composite Shell Structures

L. B. GRESZCZUK* AND R. J. MILLER†

McDonnell Douglas Astronautics Company, Santa Monica, Calif.

The high cost of advanced filamentary composites has led to the investigation and development of new design concepts for buckling-critical composite shell structures. Results are presented on structural efficiency and cost effectiveness of shells designed for buckling under external pressure and axial compression. Use of a pseudo-*T*-rib stiffening concept in which small quantities of high-modulus fibers are placed at the tip of a metal stiffener significantly increases buckling efficiency. A 10-volume-percent of boron-epoxy (as compared to the total volume of material in a stiffened metal shell) increases the buckling efficiency of an externally pressurized shell as much as 80% at a cost comparable to that of all-metal structures. Similar results are obtained for buckling-critical shells subjected to axial compression. For an integrated-composite shell consisting of an aluminum cylinder overwrapped with boron-epoxy and subjected to external pressure, the experimentally determined structural efficiency is 47% greater than that of an all-aluminum cylinder of similar geometry. It is shown that problems involving joints and attachments, which are critical for all-composite structures, are minimized through the use of new design concepts.

Nomenclature

B_x, B_y = extensional stiffness of orthotropic cylinder in axial x and hoop direction y, respectively, lb/in.
D_x, D_y = flexural stiffness of orthotropic cylinder in axial x and hoop y directions, respectively, in.-lb
D_{xy} = twisting stiffness in xy plane, in.-lb
E = modulus of elasticity, psi
G_{xy} = shear stiffness in xy plane, lb/in.
p = external pressure, psi
N_x = axial buckling load, lb/in.
$\acute{\mu}_{xy}$ = relates strain in the y direction due to normal stress in the x direction
$\acute{\mu}_{yx}$ = relates strain in the x direction due to normal stress in the y direction
μ_{xy} = relates strain in the y direction due to flexural stress in the x direction
μ_{yx} = relates strain in the x direction due to flexural stress in the y direction
h = rib height, in.

Presented as Paper 70-101 at the AIAA 8th Aerospace Sciences Meeting, New York, January 19–21, 1970; submitted March 24, 1970; revision received November 5, 1970. The authors wish to express their appreciation to R. J. Nebesar for his assistance during this program and for aiding in the fabrication of test specimens. This work was performed under the sponsorship of the McDonnell Douglas Astronautics Company—West under an independent research and development program.

* Staff Engineer, Advance Structures and Mechanical Department. Member AIAA.

† Engineer/Scientist Specialist, Advance Structures and Mechanical Department. Member AIAA.

w = rib width, in.
l = rib spacing, in.
t = shell thickness, in.
ρ = density, lb/in.^{3}

Subscripts

L = fiber direction
T = transverse direction
x = axial direction
y = hoop direction

I. Introduction

In the last decade, significant advances have been made in the development of filamentary composite materials for aerospace applications. Fibers made of such materials as S-glass, boron, silicon carbide, and graphite are now being used or considered for missile, aircraft, spacevehicle, and deep-submergence structures. The Young's moduli of these materials range from 12.4×10^6 psi for S-glass fibers to as high as 60×10^6 psi for boron fibers and 100×10^6 psi for certain graphite fibers. Tensile strengths range from 300 to 600×10^3 psi. Research is now in progress to develop and improve continuous filaments made of graphite, silicon carbide, alumina, and other materials.

In contrast to the fast pace of material development, efficient structural design concepts for filamentary materials have been rather slow to appear. Only a few existing concepts benefit fully from the inherent advantages of filamentary construction. (Two examples are isotensoid dome shapes for internal pressure vessels, described in Ref. 1, and use of optimum material layup for buckling-critical structures.) In most contemporary applications, composites are merely substituted for conventional isotropic materials, and the designs resemble those of conventional structures. This approach frequently creates serious problems, especially with joints and cutouts, and offers only limited weight savings. Because of these considerations, as well as stringent reliability requirements and the high cost of filamentary materials, designers have often been reluctant to accept composites over conventional isotropic materials.

Recent studies of new design concepts for composites have sought to obviate these adverse considerations by taking full advantage of the superior properties of the filaments and by employing the great freedom and flexibility of design and fabrication permitted by filamentary materials. Two of these new concepts are discussed here as applied to buckling-critical shell structures: the pseudo-T-rib stiffening concept and the integrated-composite concept. In both, small quantities of high-modulus composites are used to gain significant improvement in the efficiency of metal structures.

II. Background

One of the factors which deters wide-scale application of filamentary composites in aerospace structures is their high cost. Some typical cost figures for composites are shown in Table I. These figures represent recent data (1969) and apply to small quantities of purchased material (less than 5 lb). The cost of various composites is expected to decrease with time, and also with the quantity of material purchased. Nevertheless, the cost of composites is several orders of magnitude higher than the cost of such common materials as aluminum and steel. Even if the cost of the existing composites is reduced significantly, the second- and third-generation composites, when they finally emerge on the market, will undoubtedly be high-priced. It is this factor—cost—which has led to the investigation of new structural concepts for employing composites efficiently and cost-effectively.

In order to arrive at accurate conclusions, the new design concepts have been applied to structural components of vehicles which are operational today (Thor), or which will be operational in the near future (an advanced interceptor). In the case of the Thor missile, which has been operational for 10 years, the shell components are designed primarily for buckling under axial compression; the design employs waffle construction.

In the case of an advanced interceptor discussed here, the shell components are designed for buckling under external pressure. A representative configuration used in this study is an aluminum elliptical cylinder stiffened with elliptical Z frames. The existing design has been optimized for rib geometry, rib spacing, and skin thickness so that the over-all and local buckling (buckling between the frames) occur simultaneously, and the structure meets all other imposed requirements. Upon optimization of the all-metal structural configuration, studies were performed on the possible increases in structural efficiency due to cost-effective application of composites. Although the results presented herein are for boron-epoxy composites, the concepts apply to other types of existing composites, as well as composites not yet available.

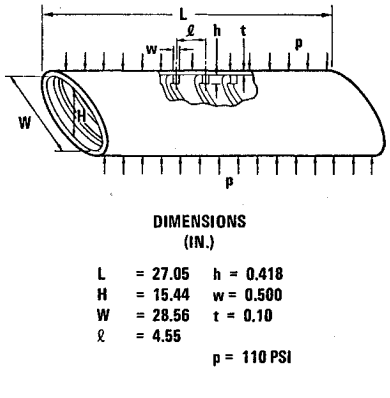

Fig. 1 Optimized all-metal configuration.

III. Pseudo-T-Rib Stiffening Concept

The shell configuration selected to illustrate the concept is shown in Fig. 1. The geometry and loading are representative of those encountered by an advanced interceptor. The structure is an elliptical, stiffened aluminum cylinder. One of the constraints imposed on the structure was that $(h+t)$ could not exceed 0.518 in. Using the equations given in the Appendix, the rib spacing and size (within the limitations stated previously) were optimized for over-all and local instability (buckling between frames). The stiffened shell was analyzed by the equivalent-stiffness, equivalent-cylinder method; that is, by smearing out the ribs and treating the ellipse as an equivalent cylinder with radius equal to the maximum radius of curvature for the ellipse. The application of equivalent-circular-cylinder theory to predict external buckling pressure for an isotropic elliptical shell yields reasonably accurate results.[2]

Following determination of the optimum geometry of a stiffened all-metal shell, the effect of the pseudo-T-rib stiffening concept on shell buckling efficiency was investigated. In this concept, boron-epoxy, or some other suitable high-modulus composite, is provided at the tip of the rib. This yields a stiffener of simple geometry that possesses stiffness equivalent to a T stiffener. Figure 2 shows the effect of the

Table 1 Cost of broad goods

Composite	Type of goods	Approximate cost, $/lb
Glass-epoxy	Resin-impregnated tape	12
Boron-epoxy	Resin-impregnated tape	500
Graphite-epoxy	Resin-impregnated tape	510
Boron-aluminum	0.020-in.-thick panels	2000

pseudo-T-rib stiffening on the buckling efficiency of an elliptical shell. As noted there, the results also apply to stiffened circular shells. Buckling pressure divided by the weight per unit surface area is plotted as a function of volume percent of boron-epoxy λ.‡ The same approach as that used to optimize the all-metal structure was used to obtain the results shown in Fig. 2 (see Appendix). The parameters W, H, L, h, t, and w were kept the same as shown in Fig. 1; only the rib spacing l and the amount of boron-epoxy at the tip of the rib were varied. The rib spacing l was varied to satisfy the over-all and local buckling requirements, that is, to ensure that the over-all and local buckling occur at the same external pressure. The modulus of elasticity of a boron-epoxy composite was taken as 40.36×10^6 psi, which corresponds to a composite with 67% fiber volume fraction.

The efficiency of the pseudo-T-rib stiffening concept is quite apparent. Approximately 4.8% boron-epoxy by volume increases the buckling efficiency by 50%, while 8.8 volume percent of boron-epoxy placed at the tip of the rib increases the buckling efficiency by 75%. As the volume fraction of boron-epoxy increases, the rate of increase in buckling efficiency decreases.

Figures 3 and 4 show the cost effectiveness of the pseudo-T-rib stiffening concept. In arriving at these figures, it was assumed that 10 shells would be built; the cost shown is per shell. Figure 3 shows the total cost of boron-epoxy prepreg required to increase the buckling efficiency over that of an all-metal structure by a given amount.§ The cost shown is for material only and represents the total material cost for a structure with the external geometry shown in Fig. 1. In Fig. 4, an attempt has been made to present the cost effectiveness of pseudo-T-rib stiffening in another way. Here, a comparison is made between cost-per-unit structural efficiency of optimized all-aluminum stiffened shells and of the shells stiffened with boron-epoxy-reinforced stiffeners. The

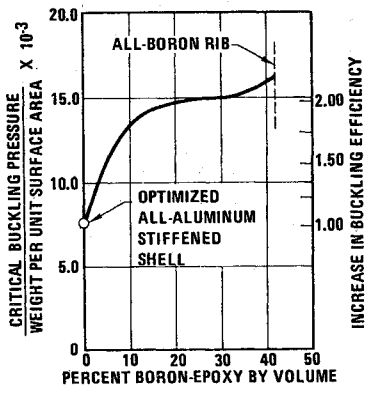

Fig. 2 Buckling efficiency of a pseudo - T - rib-stiffened elliptical cylinder.

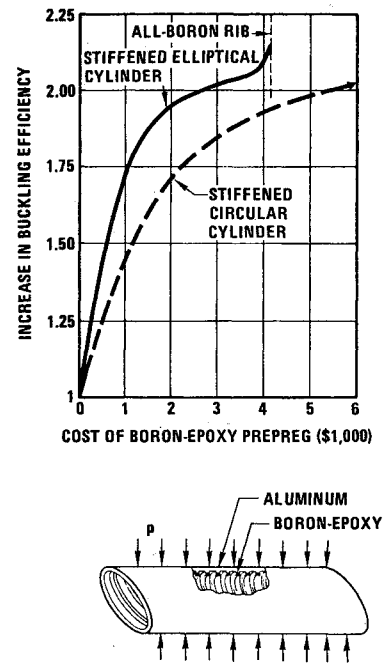

Fig. 3 Total cost of boron-epoxy prepreg to increase the buckling efficiency of stiffened cylinders subjected to external pressure.

parameter ξ which denotes the cost per unit structural efficiency, is defined as

$$\xi = \frac{(\text{Total weight of structure}) \times (\text{Cost per pound of metal structure})}{(\text{Critical buckling pressure})/(\text{Weight per unit surface area})}$$

The results shown in Fig. 4 apply to the configuration shown in Fig. 1 and include not only the cost of boron-epoxy prepreg but also estimated fabrication costs. In estimating the fabrication cost, it was assumed that the stiffeners would be of Z crosssection and that the boron-epoxy would be filament-wound on the outside of the inner Z flange, as shown in Fig. 5. In other words, the Z stiffeners themselves, supported by appropriate fixtures, would serve as mandrels. The cost included such items as fixtures for filament-overwinding the stiffeners, preparation of stiffeners, preparation of stiffeners for bonding boron-epoxy to aluminum, filament overwinding, curing, and final finishing. As before, in estimating the cost, it was assumed that 10 components would be fabricated, and the cost was amortized accordingly. (If

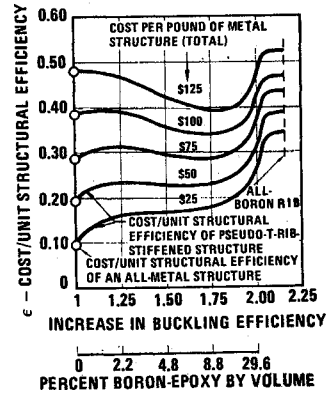

Fig. 4 Cost Efficiency of an externally pressurized, pseudo-T-rib-stiffened elliptical shell.

‡ λ is defined as volume of boron-epoxy divided by the total volume of material per unit bay.

§ These results are based on the cost of boron-epoxy prepreg shown in Table 1, with appropriate reductions in cost (obtained from Narmco Whitaker) as the amount of purchased material increases.

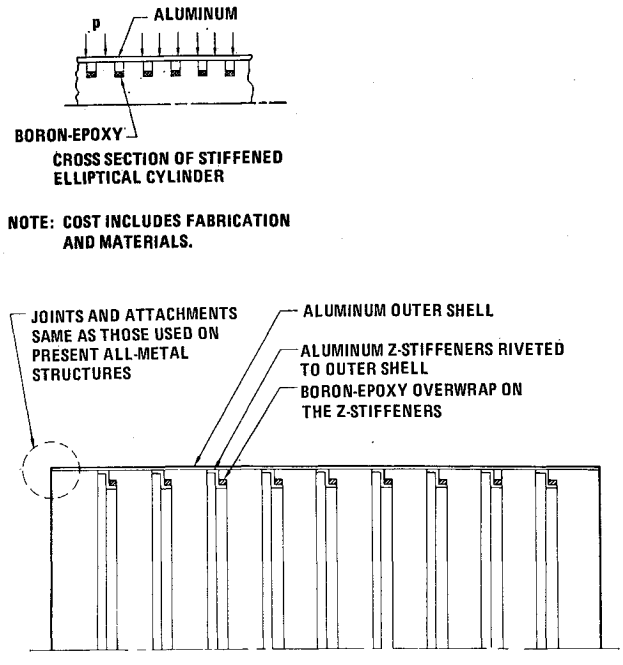

Fig. 5 Typical configuration of a pseudo-*T*-rib-stiffened shell.

more than 10 components were fabricated, the cost would decrease further, but not significantly.)

The cost figures shown in the center of Fig. 4 represent assumed cost per pound of an all-metal structure, including fabrication and materials. By multiplying the weight of the structure shown in Fig. 1 by the cost per pound of an all-metal structure, and dividing the result by the structural efficiency, one obtains the cost-per-unit structural efficiency of an all-aluminum structure. The effect of reinforcing the frames with varying amounts of boron-epoxy on the cost-per-unit structural efficiency is shown by the various curves. From the results presented in Fig. 4, it is readily seen that in terms of the variable ξ pseudo-*T*-rib stiffening permits structures that are more economical than metal structures costing \$75 or more per pound of finished product. For comparison, the cost per pound of DC-8 and Boeing 707 structures is of the order of \$40–\$60, while for missiles and space vehicles the cost per pound ranges between \$100 to \$300. The value of 1 pound of material in terms of payload can, of course, be as much as several orders of magnitude higher.

In addition to being cost-effective, other advantages of pseudo-*T*-rib stiffening are 1) the problems of joints are minimized since, as shown in Fig. 5, conventional joining techniques similar to those used for metals can be employed; 2) the boron/epoxy/aluminum stiffener possesses ductility; and 3) the concept requires a minimum amount of development, as compared to an all-composite structure.

The pseudo-*T*-rib stiffening concept is equally applicable to shells designed for buckling under axial compression. Typical results are shown in Fig. 6, where the buckling efficiency of pseudo-*T*-rib-stiffened shells is compared to the buckling efficiency of aluminum-stiffened shells. The results given are for a typical shell component of a Thor missile. Present designs utilize waffle construction. The skin thickness (t = 0.050 in.) was dictated by the internal pressure requirements, while the waffle geometry was dictated by axial compression load. The waffle has a 45° orientation with respect to the axial load. Waffle height is 0.21 in., width is 0.12 in., and spacing is 3.0 in. The waffle geometry was optimized within the limitations stated previously. This design has been verified experimentally. Test-theory correlation was within 7% (Ref. 3), with theory being higher.

The pseudo-*T*-rib stiffening concept was applied to Thor

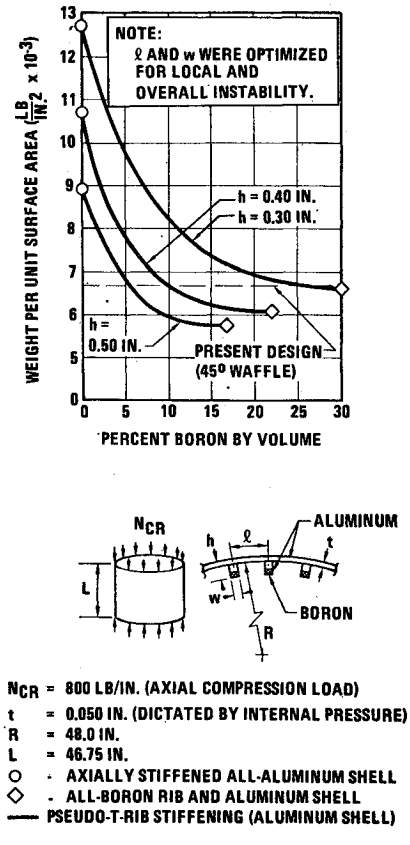

Fig. 6 Weight comparison of buckling-critical stiffened shells for a specified axial compression load.

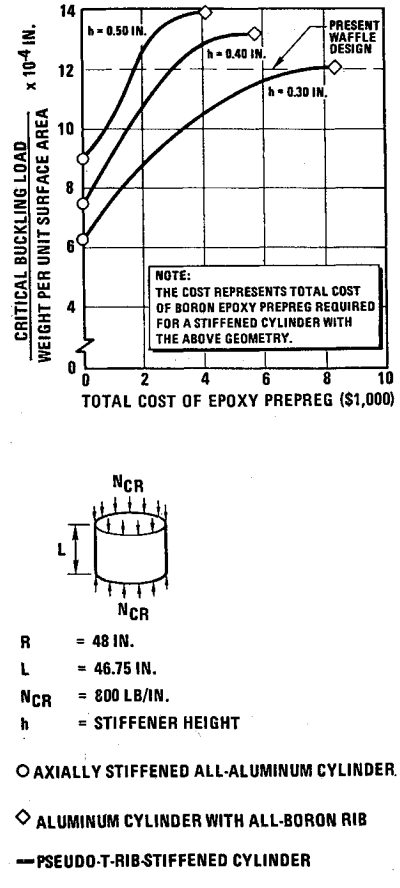

Fig. 7 Total cost of boron-epoxy prepreg to increase the bukling efficiency of stiffened cylinders subjected to axial compression.

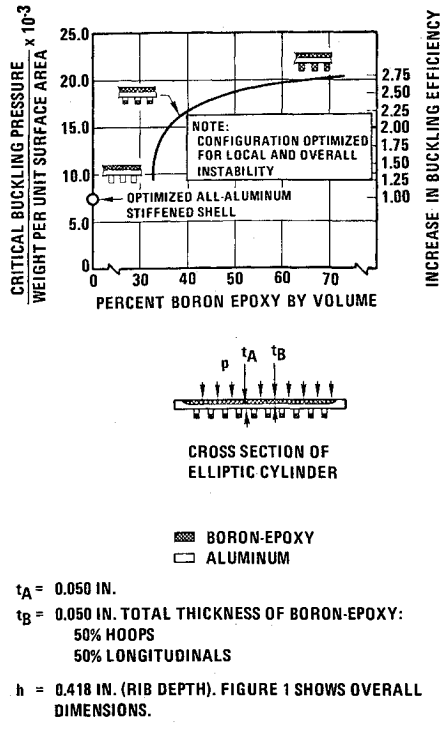

Fig. 8 Buckling efficiency of an elliptical, integrated-composite shell subjected to external pressure.

within the same limitations as stated previously. The skin was left as 0.050 in., and only the stiffener geometry, stiffener spacing, and the amount of boron-epoxy at the tips of the stiffeners were varied. The stiffener width and spacing were optimized to ensure that overall and local instability occurred at the same load. Figure 6 shows that for the given axial compression load (N = 800 lb/in.), pseudo-T-rib stiffening gives a structure weighing only 52% as much as an axially stiffened, all-aluminum shell. When compared to waffle construction, the pseudo-T-rib-stiffened structure is 14% lighter. By optimizing the orientation of boron-epoxy-reinforced stiffeners, further reduction in weight can be realized. Finally, it is readily seen that the performance of the present design can be matched by using 6% boron-epoxy at the tip of the axial stiffener. As in the case of externally pressurized shells, pseudo-T-rib stiffening appears to be a cost-effective and efficient concept for structures that are designed for buckling under axial compression. The cost of boron-epoxy required to increase the buckling efficiency is given in Fig. 7. The results presented there are for a structure of given geometry, as noted.

IV. Integrated-Composite Concept

Another method of utilizing composites efficiently is through the integrated-composite concept, in which not only the stiffeners but also the outer shell are reinforced with boron-epoxy or some other high-modulus composite. Here, too, the problems common to all-composite structures (such as joints and attachments and lack of ductility) are avoided. The addition of boron-epoxy on the outer shell further increases the buckling efficiency and also significantly increasse the axial bending stiffness, which frequently is required in advanced interceptors. Typical results on the buckling efficiency of an integrated-composite shell subjected to external pressure are shown in Fig. 8. These results were calculated using equations given in the Appendix and apply to the structure with the geometry shown in Fig. 1. Most of the discussion regarding the advantages of the pseudo-T-rib stiffening concept applies here as well. The results are based on the previously given material properties.

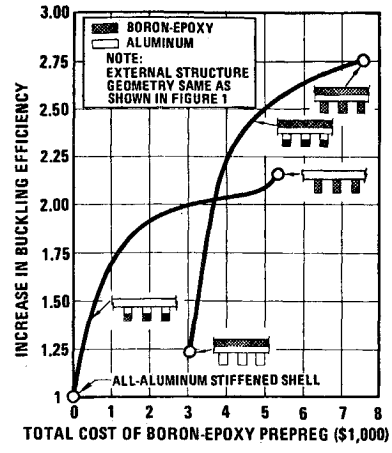

Fig. 9 Comparison of cost effectiveness of pseudo-T-rib-stiffened and integrated-composite elliptical shells.

As is apparent from Fig. 8, the external boron-epoxy overwrap on the shell is less efficient in increasing the buckling efficiency than the boron-epoxy placed at the tip of the rib. This concept is, therefore, less cost-effective than pseudo-T-rib stiffening. Figure 9 presents a rough indication of the relative cost effectiveness of pseudo-T-rib stiffening and the integrated-composite concept.

V. Experimental Investigation

A boron/epoxy/aluminum cylinder was fabricated and tested under external hydrostatic pressure to establish the efficiency of an integrated-composite concept. Using the equations given in the Appendix, tradeoff studies were performed on the effect of composite layup on external buckling pressure. The results are shown in Fig. 10 and were based on

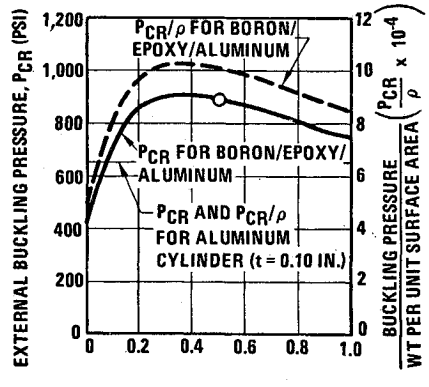

GEOMETRY OF BORON/EPOXY/ALUMINUM CYLINDER

t_H = THICKNESS OF BORON-EPOXY HOOP WRAP
t_L = THICKNESS OF BORON-EPOXY LONGITUDINAL WRAP
t_A = 0.050 IN. (THICKNESS OF ALUMINUM)
$t_H + t_L$ = 0.050 IN. (ASSUMED CONSTANT)
k = 67% (FIBER VOLUME FRACTION)

COMMON PARAMETERS FOR BORON/EPOXY/ALUMINUM AND ALUMINUM CYLINDERS

D = 6.0 IN. (INSIDE DIAMETER)
L = 10.0 IN.
t = 0.10 TOTAL WALL THICKNESS

O CONFIGURATION SELECTED FOR TESTING

Fig. 10 External hydrostatic buckling pressure for aluminum and boron/epoxy/aluminum cylinders.

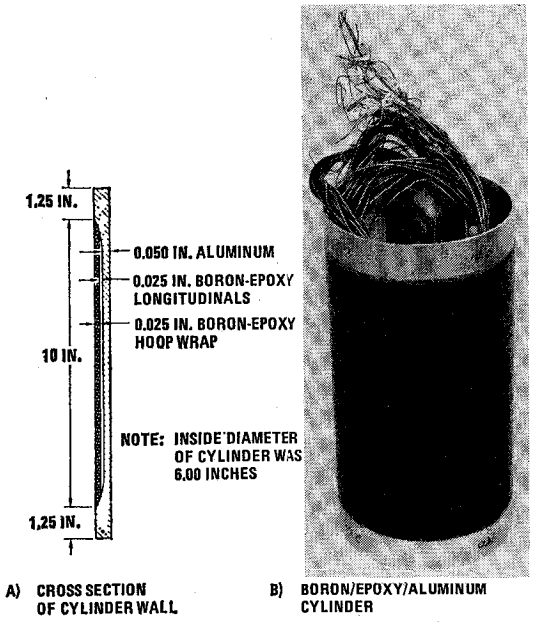

Fig. 11 Boron/epoxy/aluminum test cylinder (after test).

the following material properties:

$$\left.\begin{aligned} E_L &= 40 \times 10^6 \text{ psi} \\ E_T &= 3.5 \times 10^6 \text{ psi} \\ G_{LT} &= 1.0 \times 10^6 \text{ psi} \end{aligned}\right\} \text{ Boron-epoxy}$$

$$\left.\begin{aligned} \mu_{LT} &= 0.23 \\ \rho &= 0.076 \times \text{lb/in.}^3 \end{aligned}\right\} \text{ Boron-epoxy}$$

$$\left.\begin{aligned} E &= 10.0 \times 10^6 \text{ psi} \\ \mu &= 0.25 \\ \rho &= 0.10 \text{ lb/in.}^3 \end{aligned}\right\} \text{ Aluminum}$$

The configuration identified in Fig. 10 was selected for experimental evaluation. This configuration, although not quite optimum, was chosen because of fabrication practicality. Figure 11 shows the test specimen as well as its cross section. The test specimen was fabricated from 0.125-in. aluminum tube. First, the interior was machined to an inside diameter of 6.00 in. The exterior was then machined to an outside diameter of 6.20 in. Finally, the aluminum wall was machined to the geometry shown in Fig. 11a. At the ends, the thickness of aluminum was retained at 0.10 in. as a provision for joints and attachments. The thickness tapered from 0.10 to 0.05 in. over a 1.5-in. length. In the reduced section of the cylinder, five layers of boron-epoxy tape were hand-laid along the length of the cylinder. The cylinder was then overwrapped circumferentially with continuous boron-epoxy tape.

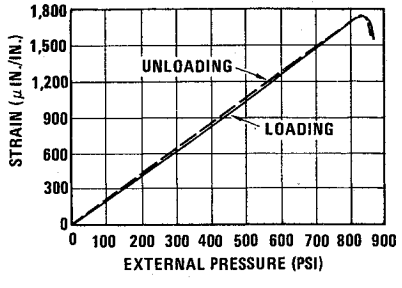

Fig. 12 External pressure vs hoop strain for boron/epoxy/aluminum cylinder (raw data).

Table 2 Comparison of buckling efficiency of aluminum and boron/epoxy/aluminum circular cylinders subjected to external pressure

Factor	Aluminum	Boron/epoxy/aluminum	Percent difference
Buckling pressure P_{CR} psi	(652)[a]	842 (890)	+29
$\frac{P_{CR}}{\text{Weight per unit area}}$	(65,200)	96,000 (101,200)	+47

[a] Numbers in parentheses are theoretical values; all others are experimental results.

The cylinder was instrumented on the inside surface with strain gages, provided with end plugs, encapsulated in a rubber sleeve, and tested under external hydrostatic pressure. Buckling occurred at 842-psi external pressure, as measured by the pressure transducer. Figure 12 shows a typical curve of measured pressure vs hoop strain. The pressure at which buckling occurred is quite obvious. The pressure was reduced gradually, and pressure vs strain readings were recorded. These values are also shown in Fig. 12. The pressure vs strain readings for loading and unloading are almost identical, indicating elastic buckling. Figure 11 shows the specimen after it was tested.

The test-to-theory correlations, as well as a comparison of buckling efficiency of boron/epoxy/aluminum and aluminum cylinders, is shown in Table 2. Since no buckling tests were performed on all-aluminum cylinders, theoretical results for aluminum cylinders were used as a basis for comparison. The buckling efficiency for a boron/epoxy/aluminum cylinder is shown to be 47% higher than that of an aluminum cylinder of similar geometry. The actual buckling pressure for an all-aluminum cylinder would be expected to be somewhat lower than the predicted value; therefore, the true buckling efficiency of a boron/epoxy/aluminum cylinder would be expected to be higher than 47%. The agreement between the experimentally and theoretically predicted buckling pressures for the boron/epoxy/aluminum cylinder is quite good. It is noted here that the equations used in the theoretical prediction are those given in the Appendix. Thus, by using the integrated-composite concept, the usual problems associated with high-modulus composite structures, such as lack of ductility, joints and attachments, and high cost, are minimized.

VI. Conclusions

By judicious reinforcement of metals with high-modulus composites, significant increases can be achieved in the buckling efficiency of stiffened metal shells subjected to axial compression or external pressure. Through this approach, the common deficiencies of composites (such as high cost, lack of ductility, and the problems of joints and attachments) can be bypassed. The concept that is particularly attractive from the standpoint of increased structural efficiency and cost effectiveness is the pseudo-T-rib stiffening concept. The experimental results further verify the validity of existing theory for predicting buckling of externally pressurized orthotropic shells and also demonstrate the structural efficiency of boron/epoxy/aluminum cylinder as compared to that of an all-aluminum cylinder.

Appendix: Buckling Equations

The classical small deflection theory was used to obtain a modified Donnell buckling solution for orthotropic cylinders. The solution for the problem is given in numerous references.[4–5]

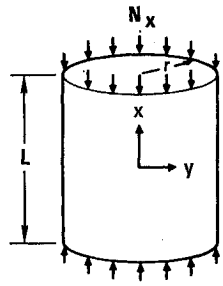

Fig. 13 Cylinder subjected to axial compression.

Buckling under Axial Compression

Critical buckling loads for all ranges of buckling of a cylinder under axial compression, assuming simply supported edges (Fig. 13), are given in (Ref. 4).

$$N_x = (K_x \pi^2 D_x)/L^2(1 - \mu_{xy}\mu_{yx}) \tag{A1}$$

where

$$K_x = m^2\left[1 + 2\left(\mu_{yx} + \frac{D_{xy}}{D_x}(1 - \mu_{xy}\mu_{yx})\right)\beta^2 + \frac{D_y}{D_x}\beta^4\right] + \frac{Z_x^2}{\pi^4}\frac{1}{m^2}\left\{\frac{1}{\left[1 - 2\left(\dot{\mu}_{yx} - \frac{B_y}{2G_{xy}}\right)\beta^2 + \frac{B_y}{B_x}\beta^4\right]}\right\}$$

$$Z_x^2 = (L^4/r^2)(B_y/D_x)(1 - \mu_{xy}\mu_{yx})$$

and β is the ratio of half-wavelength in the axial direction to hoop direction. The number of half-waves in the axial direction is given by m, and the number of half-wavelengths in the hoop direction is given by n.

Buckling under External Pressure

Critical buckling pressure for all ranges of buckling, except for a very long cylinder region, of a cylinder with simply supported edges under external pressure (Fig. 14) is given by (Ref. 5).

$$P_{cr} = K_y \pi^2 D_y/L^2(1 - \mu_{xy}\mu_{yx})r \tag{A2}$$

K_y is defined differently for external radial pressure and external hydrostatic pressure.
For external radial pressure

$$K_y = m^2\left\{\frac{D_x}{D_y}\frac{1}{\beta^2} + 2\left[\mu_{xy} + \frac{D_{xy}}{D_y}(1 - \mu_{xy}\mu_{yx})\right] + \beta^2\right\} + Z_y^2\Big/\pi^4 m^2\left[\frac{B_x}{B_y}\beta^2 - 2\left(\dot{\mu}_{xy} - \frac{B_x}{2G_{xy}}\right)\beta^4 + \beta^6\right]$$

and for external hydrostatic pressure

$$K_y = m^2\left[\frac{D_x}{D_y}\frac{1}{(\frac{1}{2} + \beta^2)} + 2\left(\mu_{xy} + \frac{D_{xy}}{D_y}(1 - \mu_{xy}\mu_{yx})\right)\frac{\beta^2}{(\frac{1}{2} + \beta^2)} + \frac{\beta^4}{(\frac{1}{2} + \beta^2)}\right] + \frac{Z_y^2}{\pi^4 m^2}\left\{\frac{1}{(\frac{1}{2} + \beta^2)\left[\frac{B_x}{B_y} - 2\left(\dot{\mu}_{xy} - \frac{B_x}{2G_{xy}}\right)\beta^2 + \beta^4\right]}\right\}$$

where β is the ratio of half-wavelength in the longitudinal direction to hoop direction and $Z_y^2 = (L^4/r^2)(B_x/D_y)\cdot(1 - \mu_{xy}\mu_{yx})$ and L is defined as the distance between supports.

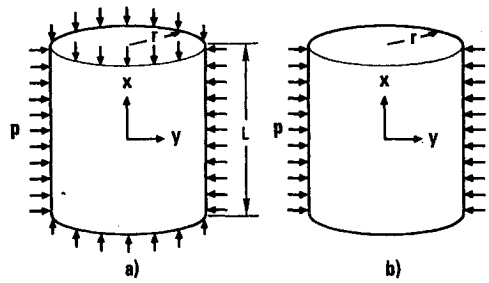

Fig. 14 Cylinders subjected to a) external hydrostatic pressure and b) external radial pressure.

Method of Minimizing

Buckling solutions were found from the previous equations by inputting into the computer program the cylinder dimension and the elastic properties of each material. From the elastic properties of each material, the elastic stiffness properties of the over-all cylinders were computed. The buckling loads were then determined by numerically minimizing the previous equations by searching through combinations of values for m and n until the lowest value of buckling load was determined. The effect of the ribs was included by assuming that the ribs had zero shear stiffness, and the elastic modulus of the ribs transverse to the direction of the ribs was taken as zero. Poisson's effect was also taken as zero. The elastic modulus in the direction of the rib was reduced by the ratio of rib width to rib spacing. If the rib contained a combination of aluminum and boron-epoxy, each modulus value was reduced in proportion to its own modulus to give the correct value for flexural stiffness, which would not occur if an average modulus was assumed for the rib without compensating for the shift in the neutral axis.

Local and Over-All Buckling

Both local and over-all buckling values of the cylinders were checked. Local buckling for the radial and hydrostatic pressure cases was checked by using the previous equations with the length between ribs as the effective cylinder length. The axial compression cylinders were checked for local buckling by using Eq. (A3).

$$N = 5.73Et^3/(1 - \mu^2)l^2 \tag{A3}$$

A buckling solution for various conditions of end restraint is given in Ref. 6.

References

[1] Read, W. S., "Equilibrium Shapes for Pressurized Fiberglas Domes," *Transactions of the ASME, Ser. B: Journal of Engineering for Industry*, Vol. 85, 1963, pp. 115–118.

[2] Yao, J. C. and Jenkins, W. C., "Buckling of Elliptic Cylinders Under Normal Pressure," AIAA Paper 70-105, New York, 1970.

[3] Meyer, R. R., "Buckling of Eccentric-Stiffened Waffle Cylinders," *Journal of the Royal Aeronautical Society*, Vol. 71, 1967, pp. 516–520.

[4] Schneider, M. H., "Buckling of Fiberglass Cylinders Under Axial Compression," SM-43514, May 1964, Douglas Aircraft Co., Santa Monica, Calif.

[5] Schneider, M. H. and Hofeditz, J. T., "Buckling of Fiberglass Cylinders Under External Pressure," Preprint 64-WA/UNT-12, Dec. 1964, the American Society of Mechanical Engineers, New York.

[6] Cheng, S. and Ho, B. P. C., "Stability of Heterogeneous Aelotropic Cylindrical Shells Under Combined Loading," *AIAA Journal*, Vol. 1, No. 4, April 1963, pp. 892–898.